BBA - Molecular Basis of Disease 1870 (2024) 166911

Contents lists available at ScienceDirect

BBA - Molecular Basis of Disease

journal homepage: www.elsevier.com/locate/bbadis

Dectin1 contributes to hypertensive vascular injury by promoting macrophage infiltration through activating the Syk/NF-κB pathway

Jiajia Zhang [a,b,c,1], Yu Tu [a,b,c,1], Jiajia Wei [a], Ruyi Zheng [a], Ji Shao [a], Qinhua Chen [d], Guang Liang [a,b], Huazhong Ying [a,b,c,*], Xue Han [a,b,*], Qiaojuan Shi [a,b,c,*]

[a] Zhejiang Provincial Key Laboratory of Laboratory Animals and Safety Research, Hangzhou Medical College, Hangzhou 310013, China
[b] Zhejiang TCM Key Laboratory of Pharmacology and Translational Research of Natural Products, Hangzhou Medical College, Hangzhou 310013, China
[c] Engineering Research Center of Novel Vaccine of Zhejiang Province, Hangzhou Medical College, Hangzhou 310013, China
[d] Key Laboratory of TCM Clinical Pharmacy, Shenzhen Baoan Authentic TCM Therapy Hospital, Guangzhou University of Chinese Medicine, Shenzhen 518101, China

ARTICLE INFO

Keywords:
Dectin1
Vascular injury
Inflammatory response
Nuclear factor kappa B
Macrophages

ABSTRACT

Vascular injury is an early manifestation leading to end-organ damage in hypertension pathogenesis, which involves a macrophage-associated immune response. Dendritic cell-associated C-type lectin-1 (Dectin1) is a pivotal player in regulating inflammation-mediated cardiovascular disease. However, its role in hypertension-induced vascular damage and the underlying mechanisms remain unclear. We hypothesized that Dectin1 might accelerate angiotensin II (Ang II)- or deoxycorticosterone acetate–salt (DOCA-salt)-induced vascular injury through proinflammatory actions in macrophages. Macrophage Dectin1 was upregulated in mouse aortic tissues stimulated with Ang II. In the peripheral blood, Ang II also increased $CD11b^{+}F4/80^{+}$ macrophages in mice. In our constructed Dectin1 knockout mice, Dectin1 deletion protected against Ang II-induced EB extravasation and aortic wall thickness. Deficiency of Dectin1 or its pharmacological inhibition considerably improved fibrosis and inflammation responses, accompanied by a reduction in M1 macrophage polarization as well as proinflammatory cytokines and chemokines induced by Ang II or DOCA-salt. Through the bone marrow (BM) transplantation assay, these effects were verified in the wild type mice reconstituted with Dectin1-deficient BM cells. Mechanistically, Ang II promoted Dectin1 homodimerization, thereby triggering the spleen tyrosine kinase/nuclear factor kappa B pro-inflammatory cascade to induce the expression of inflammatory factors and chemokines *in vivo* and *in vitro*. In conclusion, Dectin1 has an essential role in the pathogenic procedure of Ang II-stimulated or DOCA-salt-induced vascular damage in mice and represents a promising therapeutic target for cardiovascular diseases.

1. Introduction

Vascular injury, a major complication of hypertension, is an early manifestation of hypertension-induced end-organ damage [1]. It is linked with many cardiovascular diseases, including atherosclerosis and myocardial infarction [2,3]. Increasing number of studies have indicated that multiple factors, including but not limited to the renin–angiotensin–aldosterone system, endothelin system, and genetic predisposition, collectively or individually contribute to an elevation in blood pressure and subsequent cardiovascular injury [4,5]. Currently, the efficacy of molecular pathways in guiding hypertension treatment has been clearly demonstrated in clinical practice, but vascular injury-targeting drugs are still under study [6]. Therefore, a deeper understanding of the processes could facilitate the development of effective preventive and therapeutic strategies.

Accumulating evidence has revealed that inflammation is an essential component in vascular damage progression under hypertension pathogenesis [4,5,7]. An increase synthesis and release of adhesion molecules, chemokines, and cytokines is induced by immune cell infiltration, especially infiltration of monocytes and macrophages, which has been linked to cardiovascular damage [8,9]. Angiotensin II (Ang II)-induced hypertension has been proven to be reliant on the presence of $CD11b^{+}F4/80^{+}$ M1 macrophages [7]. Monocytes/macrophages are also implicated in the pathophysiology of the hypertensive disease and organ

* Corresponding authors at: Zhejiang Provincial Key Laboratory of Laboratory Animals and Safety Research, Hangzhou Medical College, Hangzhou 310013, China.
E-mail addresses: yhz0101@126.com (H. Ying), 13819113623@163.com (X. Han), shiqiaojuan@163.com (Q. Shi).
[1] These authors contributed equally to this work.

https://doi.org/10.1016/j.bbadis.2023.166911
Received 13 June 2023; Received in revised form 13 September 2023; Accepted 2 October 2023
Available online 9 October 2023

damage in the deoxycorticosterone acetate-salt (DOCA-salt) model [10,11]. Moreover, a favorable correlation was observed between the occurrence of cardiovascular events and the increase in the number of circulating $CD14^+$ M1 macrophage [12]. Accordingly, interfering with the polarization of proinflammatory M1 macrophages may attenuate the inflammatory process and prevent vascular injury in hypertension.

Dendritic cell-associated C-type lectin-1 (Dectin1) acts as a transmembrane pattern recognition receptor and belongs to the c-type lectin-like superfamily. Specifically, Dectin1 is expressed by myeloid-monocytic cells such as macrophages [13]. Dectin1 stimulates intracellular signaling through immunoreceptor tyrosine-based activation motif-like (ITAM-like) motifs that subsequently recruit and activate spleen tyrosine kinase (Syk), ultimately resulting in nuclear factor kappa B (NF-κB) activation [14,15]. Dectin1 has been most studied in the context of antifungal defense through its ability to recognize β-glucans [16]. However, recent studies have demonstrated its wider role in non-pathogen-mediated sterile inflammation [17]. Indeed, Dectin1 is essential for regulating cardiac inflammation [18], respiratory [19], intestinal [20], neurological [21], and developmental disorders. Dectin1 plays a crucial role in encouraging cardiac inflammation and dysfunction, following mouse myocardial IR damage [22]. In addition, our recent study demonstrated that Dectin1 overexpression caused macrophage polarization and contributed to cardiac inflammation and remodeling [23]. These findings imply that Dectin1 is of significance for the emergence of hypertension-associated cardiovascular diseases. However, the detailed molecule mechanisms remain unelucidated.

We hypothesized that Dectin1 exacerbated hypertensive vascular injury. To verify this hypothesis, we first evaluated whether genetic deletion or pharmacological inhibition of Dectin1 could protect against Ang II- or DOCA-salt-induced vascular injury by suppressing M1 macrophage infiltration *in vivo*. Moreover, detailed mechanistic studies of macrophages were conducted to determine whether this protective effect was achieved by inhibiting Syk/NF-κB signaling pathways and reducing inflammatory cytokine production *in vivo* and *in vitro*.

2. Materials and methods

2.1. Animals

Six-week-old male C57BL/6 mice (weight: 18–22 g) were obtained from the Hangzhou Medical College's Laboratory Animal Centre (Hangzhou, China). The male Dectin1 knockout (D1KO) mice in the C57BL/6 genetic background and male littermates of wild type (WT) mice weighting 18–22 g were a gift from Professor Guang Liang from Wenzhou Medical University (Wenzhou, China). The mice were housed in a controlled setting with a 12 h:12 h light–dark cycle (23–26 °C, 40 %–60 % humidity). All mice received free access to a typical rodent diet. Experimental methods used for animal investigations were authorized by the Ethics Committee of Laboratory Animal Care and Welfare, Hangzhou Medical College (approval number: ZCLA-ACUC-20030058). The National Institutes of Health's Guidelines for the Care and Use of Laboratory Animals were followed during these operations.

2.2. Aorta injury model caused by hypertension

A micro-osmotic pump (cat. no. Alzet MODEL 1004, CA, USA) containing Ang II (1.44 mg/kg/day; cat. no. A107852, Aladdin, Shanghai, China) was implanted subcutaneously in a mouse model of aortic damage. The pumps were placed on the back of the WT and D1KO mice under isoflurane anesthesia for 28 days, as previously reported [24,25]. Following pump installation, the mouse wounds were cleaned, and 1 g/L neomycin was introduced into their water supply.

A different hypertension model was used to generate the aortic damage [26]. The WT and D1KO mice were subcutaneously implanted with DOCA (50 mg; Innovative Research of America, USA) pellets and received 1 % saline in drinking water for 3 weeks.

Systolic blood pressure (SBP) and diastolic blood pressure (DBP) were recorded every 7 days between 1:00 pm and 5:00 pm using a tail-cuff Pressure Analysis System (BP-98A, Softron Biotechnology, Tokyo, Japan). An accurate recording was the average of 10 measurements for each mouse.

2.3. Experimental protocols

In the Ang II-induced vascular injury model, the mice were randomly assigned to 5 experimental groups ($n = 7$/group): (i) both untreated WT mice and (ii) untreated D1KO mice received 0.9 % saline solution (WT-Ctrl and D1KO-Ctrl, respectively); (iii) Ang II-infused WT mice and (iv) Ang II-infused D1KO mice received 0.9 % saline solution (WT-Ang II and D1KO-Ang II, respectively); and (v) Ang II-infused WT mice treated with laminarin (300 mg/kg; cat. no. L9634, Sigma-Aldrich Chemie GmbH, Taufkirchen, Germany; WT-Ang II-Laminarin). Laminarin, a type of Dectin1 inhibitor, was administered intraperitoneally once every other day [27].

In the DOCA-salt-induced vascular damage model, the mice were divided into five groups at random ($n = 7$/group): (i) both untreated WT mice (WT-Ctrl) and (ii) untreated D1KO mice (D1KO-Ctrl); (iii) the DOCA pellet-implanted WT mice (WT-DOCA) and (iv) D1KO mice (D1KO-DOCA) given water containing 1 % saline; and (v) the DOCA pellet-implanted WT mice given water containing 1 % saline treated with laminarin (300 mg/kg; *i.p.*; WT-DOCA-Laminarin).

All mice survived the experimental duration. Following the trial, the mice were euthanized with sodium pentobarbital (*i.p.*; 50 mg/mL) under anesthesia. Blood samples were collected and serum was prepared for measuring Ang II (cat. no. SEA007Mu, Wuhan cloud clone technology, China), tumor necrosis factor (TNF)-α (cat. no. MEC1003, Anogen, Canada), and interleukin 6 (IL-6) (cat. no. MEC1008, Anogen) using enzyme-linked immunosorbent assay (ELISA) kits. Aortic tissues were harvested for paraffin embedding or snapped frozen in liquid N_2 for mRNA and protein expression analysis.

2.4. Bone marrow transplantation experiment

Six-week-old male WT or D1KO mice were selected as donors, and bone marrow (BM) cells were extracted from their femurs and tibias. Briefly, these mice were sacrificed and placed in a beaker containing 75 % ethanol for immersion disinfection. The isolated femurs and tibias were placed in Dulbecco's modified Eagle's medium (DMEM; Gibco, Eggenstein, Germany) supplemented with 10 % fetal bovine serum (FBS; Gibco). The bone cavity was irrigated multiple times using a 1-mL syringe. The cells were harvested, centrifuged at 1000 rpm for 5 min, and reconstituted in phosphate-buffered saline (PBS) for counting.

Male four-week-old D1KO or WT mice were selected as recipients. These mice were housed with ultrapure water containing 2 g/L neomycin before transplantation. The recipient mice were systemically irradiated (6 Gy). After 9 h, 5×10^6 BM cells were transferred into the recipient mice through the tail vein. For 3 weeks following transplantation, the recipient mice were continuously fed with ultrapure water containing neomycin (2 g/L). Through RT-qPCR or agarose gel electrophoresis of DNA, the tails, aortas, BM cells, and peripheral blood mononuclear cells of recipient mice were evaluated to determine whether BM transplantation (BMT) was successful.

2.5. Histological analysis

The aorta samples were fixed, immersed in paraffin, and sliced into 5-μm-thick slices. Hematoxylin–eosin (H&E) staining was performed to examine the morphology of the sections, such as the aortic nucleus and wall thickness. The identification of aortic fibrosis on Masson's trichrome staining was observed under a bright-field microscope (magnification: 200×; Leica, Wetzlar, Germany). In addition, the collagen deposition on the Sirius red-stained sections was evaluated under the

bright-field microscope and a polarizing microscope (magnification: 200×; Nikon Eclipse Ci, Tokyo, Japan).

The paraffin was applied to the tissues before immunohistochemical staining. The slides were oven dried at 65 °C for 20 min and deparaffinized. Antigen retrieval was performed in citrate buffer by heating the sections for 8 min at 65 °C. Following a 25-min exposure to 3 % hydrogen peroxide solution at 25 °C, the slides were blocked for 1 h with 5 % bovine serum albumin (BSA). The slices were then incubated with primary antibodies for an additional night at 4 °C: F4/80 (1:300, cat. no. MCA497R, Bio-Rad Laboratories, CA, USA), TNF-α (1:300, cat. no. sc-52746, Santa, USA), CD86 (1:300, cat. no. 91882, Cell Signaling Technology, USA), CD206 (1:300, cat. no. 18704-1-AP, Proteintech, China), TGF-β (1:300, cat. no. ab92486, Abcam, UK), and COL-1 (1:500, cat. no. sc-59772, Santa, USA). Finally, a secondary antibody conjugated to horseradish peroxidase (HRP) (1:300, Servicebio, Wuhan, China) was added and incubated for 50 min at 25 °C. Immunoreactivity was determined using diaminobenzidine (Servicebio). Images were obtained under a bright-field microscope (magnification: 25× and 200×).

2.6. Evans blue staining

The mice were injected 2 % solution of the Evans blue (EB) dye in saline through the tail vein 30 min before tissue collection. During tissue collection, EB in the blood was effectively eliminated by injecting saline through the left ventricle and draining the dye through the right atrial appendage, followed by perfusion fixation with 4 % neutral buffered formalin. The aortic tissue was meticulously dissected. The vascular integrity was evaluated quantitatively by determining EB extravasation. The photographs were evaluated using ImageJ software (NIH, Bethesda, MD, USA).

2.7. Immunofluorescence staining

For immunofluorescence staining, the sections were subjected to the aforementioned processing steps and were left at 4 °C overnight in a mixture containing Dectin1 (1:100, cat. no. ab140039, Abcam) and CD68 (1:300, cat. no. 66231-2-Ig, Proteintech, China) or Dectin1 (1:100) and CD31 (1:300, cat. no. AF3628, R&D SYSTEMS, Germany). Following washing in PBS, the sections were incubated with Cy3-conjugated donkey antirabbit IgG (1:300, cat. no. GB21403, Servicebio), Alexa Fluor® 488-conjugated goat antimouse IgG, and Alexa Fluor® 488-conjugated donkey antigoat IgG for 50 min at 25 °C. The slides were cleaned with PBS, stained for 10 min with DAPI, and mounted using the antifluorescence quenching blocking reagent. Using a confocal microscope (Nikon, Japan; A1R-SIM-STORM, magnification: 200×), images were captured.

2.8. Flow cytometry

The presence of $CD11b^{+}F4/80^{+}$ macrophages within the mouse peripheral blood was assessed through flow cytometry. In brief, 100 μL peripheral blood was collected and placed in an anticoagulant tube. The samples were stained with an antibody mixture for 45 min at 4 °C in the dark. The following antibodies were employed: CD11b-PerCP/Cyanine5.5 (1:100, cat. no. 45-0112-80, eBioscience, CA, USA) and F4/80-PE (1:100, cat. no. 12-4801-80, eBioscience). After staining, red blood cell lysis buffer (cat. no. C3702, Beyotime Biotechnology, Shanghai, China) was added to the cells, and the process was repeated twice. The cells were then washed in PBS, spun at 400 *g* for 5 min, and resuspended in 300 μL of PBS. The single cells were ultimately examined using FACSCelesta equipment (BD Biosciences, San Jose, CA, USA). The data were analyzed using FlowJo V10 software (Tree Star, USA).

2.9. Cell cultures and treatment

RAW264.7 (murine monocyte–macrophage leukemia cells), vascular smooth muscle cells (VSMCs), human aortic fibroblasts (HAFs), and human umbilical vascular endothelial cells (HUVECs) were supplied by Shanghai Institute of Biochemistry and Cell Biology (Shanghai, China). The DMEM medium containing 10 % FBS and with no sodium pyruvate was used to cultivate RAW264.7 cells. The low-glucose DMEM medium supplemented with 10 % FBS was used to cultivate VSMCs. The fibroblast medium (Sciencell, Carlsbad, CA, USA) was used to cultivate HAFs. This medium contains 2 % FBS and 1 % fibroblast growth serum (Sciencell). HUVECs were cultured in 10 % FBS-DMEM medium. The cells were placed in a 5 % CO_2 incubator at 37 °C.

Dimethyl sulfoxide (DMSO) was used to dissolve laminarin (250 mg/mL). As a vehicle, DMSO was accepted by the control cells. The RAW264.7 cells were pretreated with laminarin (300 μg/mL) for 1 h. Then, the cells were treated with Ang II (dissolved in DMSO) for 2 or 9 h at a final concentration of 1 μM. The cells were harvested for western blot or RT-qPCR analyses.

2.10. Dectin1 gene silencing

siRNA was transfected into the RAW264.7 cells to silence Dectin1. Mouse Dectin1 siRNAs (forward: 5′-GGGAAGAGCUGUUACCUAUTT-3′; reverse: 5′-AUAGGUAACAGCUCUUCCCTT-3′) were acquired from GenePharma (Shanghai, China). The negative control was a scrambled siRNA. The cells were transfected with jetPRIME (cat. no. 114-15, Polyplus-transfection® SA, Strasbourg, France). Briefly, 7 μg siRNA or scrambled control was diluted with 500 μL jetPRIME buffer, added to the 14 μL jetPRIME reagent. After being vortexed, the mixture was kept at 25 °C for 10 min. The mixture was added to the fresh medium-filled plate, which was then transfected for 6 h. The media was finally changed to full growth media for a further 28 h. Knockdown efficiency was determined on the basis of protein levels.

2.11. Mouse primary peritoneal macrophage culture

Mouse primary peritoneal macrophages (MPMs) were produced using 6-week-old C57BL/6 WT mice and age-matched D1KO mice. Briefly, the 6 % thioglycolate solution was composed of 6 g soluble starch (cat. no. LP0042, OXOID, Basingstoke, UK), 0.5 g sodium chloride (cat. no. A501218, Sangon Biotechnology, Shanghai, China), 1 g tryptone (cat. no. G8300, Solarbio, Beijing, China), and 0.3 g beef extract (cat. no. G8270, Solarbio) dissolved in 100 mL double distilled water. Each mouse was injected intraperitoneally with 4 mL of the broth and was fed normally for 48 h. Next, the animals were sacrificed, and their peritoneal cavities were rinsed with 10 mL of RPMI 1640 medium for obtaining the cell suspension. The cells were separated through centrifugation for 5 min at 1000 rpm. The cells were resuspended in 10 % FBS-RPMI 1640 medium and then planted at 5×10^4 cells per well in 24-well plates. Fresh medium was added after 2 h, and the cells were then cultured for 24 h.

2.12. RT-qPCR analysis

Total RNA was taken out of mouse aortas or cultured cells using TRIZOL (Takara, Otsu, Japan). The RNA was reverse transcribed using Hifair® III 1st Strand cDNA Synthesis SuperMix (YEASEN, Shanghai, China). On the CFX96 System (Bio-Rad, California, USA), RT-qPCR was executed using SYBR Green Master Mix (YEASEN). Primers for genes, including IL-6 (*Il6*), TNF-α (*Tnfα*), C motif ligand-2 (*Ccl2*), *Ccl5*, C-X-C motif chemokine 10 (*Cxcl10*), intercellular adhesion molecule-1 (*Icam1*), inducible nitric oxide synthase (*Inos*), arginase 1 and 2 (*Arg1* and *Arg2*), macrophage mannose receptor 1 (*Cd206*), collagen type 3 chain 1 (*Col3a1*), and transforming growth factor-beta 1 (*Tgfβ*), were provided by Sangon Biotech (Shanghai, China). In Supplementary Table 1, the primer sequences employed are provided. Target mRNA data were calculated using the $2^{-\Delta\Delta Ct}$ method and normalized by the level of *β-actin*.

2.13. Western blotting

A cell and tissue total protein extraction kit (Kang Cheng Bioengineering, Shanghai, China), along with a protease inhibitor cocktail (Biosharp, Hefei, China) and a phosphatase inhibitor cocktail (Servicebio), was applied to extract the complete proteins. After the protein was lysed, the quantities of total or fractionated protein were measured using the BCA protein assay kit (Beyotime). SDS-polyacrylamide gel electrophoresis was used to size-fractionate the protein samples before electrotransferring them onto polyvinylidene fluoride membranes. The membranes were blocked with 5 % non-fat dried milk or 5 % BSA for 1 h before incubation with specific primary antibodies overnight at 4 °C. Dectin1 (1:1000; cat. no. ab140039) was obtained from Abcam. Phospho–Syk (1:1000; cat. no. 2717), Syk (1:1000; cat. no. 13198), and phospho–IκB (1:1000; cat. no. 2859) were purchased from Cell Signaling Technology (USA). IκB (1:1000; cat. no. 10268-1-AP), NF-κB p65 (1:1000; cat. no. 10745-1-AP), LaminB (1:1000; cat. no. 66095-1-Ig), and GAPDH (1:1000; cat. no. 60004-1-Ig) were bought from Proteintech. The membranes were incubated for 2 h with HRP-conjugated secondary antibodies (1:3000, Servicebio). A chemiluminescence kit (Servicebio) was used to visualize the bands, and ImageJ was used to analyze the band densities. The loading control proteins used were LaminB or GAPDH.

2.14. Statistical analysis

Every experiment was blinded and randomized. Data were presented as means ±standard error of the mean. Independent sample *t*-test was applied to compare two groups. To determine the significance of differences among more than two groups, a one-way ANOVA was performed, followed by a multiple comparison test using Tukey. GraphPad Prism 8.0 software (San Diego, CA, USA) was applied to perform statistical analyses. At $P < 0.05$, it was declared significant.

3. Results

3.1. Expression of macrophage Dectin1 is elevated in the aortic tissues of Ang II-treated mice

To validate the involvement of Dectin1 in aortic injury model induced by Ang II, we first investigated Dectin1 expression levels in aortic tissues through western blotting and RT-qPCR. At both protein and mRNA levels, Dectin1 expression was higher in the aortas of Ang II-infused mice than in those of the control animals (Fig. 1A–C). As reported previously [28], Dectin1 is abundantly expressed in myeloid-lineage cells such as macrophages. Therefore, we predicted that macrophages were the primary source of elevated Dectin1 levels in aortic tissues. Notably, following Ang II infusion, the percentages of $CD11b^{+}F4/80^{+}$ macrophages in the peripheral blood significantly increased (Fig. 1D, E).

Correspondingly, the double-immunofluorescence staining assay further revealed that Dectin1 was markedly elevated in the aortas of Ang II-induced mice. Dectin1 was colocalized with CD68, a macrophage marker, rather than CD31, an endothelial cell marker (Fig. 1F, G, Supplementary Fig. S1A, B). Moreover, we assessed Dectin1 protein levels in cultured HUVECs, VSMCs, HAFs, RAW264.7 cells, and MPMs. Dectin1 was robustly expressed in RAW264.7 and MPM cells, where barely any expression was observed in HUVECs, VSMCs, and HAFs (Supplementary Fig. S1C, D). These findings imply that Ang II causes CD68-positive macrophages in the mouse aorta to express a higher level of Dectin1.

3.2. Dectin1 deficiency prevents aortic damage and fibrosis caused by Ang II in mice

We used the D1KO mice to investigate the involvement of Dectin1 in Ang II-induced aortic impairment and fibrosis. The successful ablation of Dectin1 expression was confirmed in the D1KO mice-derived MPMs compared with the WT mice-derived MPMs (Supplementary Fig. S2A, B). The WT and D1KO mice were implanted with subcutaneous pumps containing Ang II for a 4-week perfusion (Fig. 2A). Laminarin, a pharmacological Dectin1 inhibitor, was administered (300 mg/kg) every two days (Fig. 2A). Serum Ang II, SBP, and DBP levels were both dramatically increased in the WT and D1KO mice in response to Ang II stimulation (Fig. 2B, C and Supplementary Fig. S2C). To assess the barrier function of the vasculature, the aortic tissues of the mice were stained with the EB dye. As shown in Fig. 2D and E, compared with the aortas of the WT mice, the number of positive staining regions was noticeably increased in the Ang II-infused mice's aorta. However, the Ang II-exposed D1KO mice exhibited markedly attenuated EB extravasation. H&E staining demonstrated that Dectin1 deficiency noticeably decreased the aortic wall thickness in the Ang II-induced mice (Fig. 2F, G). Similarly, laminarin administration reduced EB extravasation and the aortic wall thickness (Fig. 2D–G). Additionally, in the Ang II-challenged WT mice, but not in the D1KO mice, *Tgfβ* and *Col3a1* mRNA levels were dramatically increased (Fig. 2H). In the aortic tissues of the Ang II-treated WT mice, Masson's trichrome and Sirius red staining revealed substantial increases in fibrosis and collagen deposition. However, in Ang II treated D1KO mice, these structural modifications were greatly attenuated (Fig. 2I–M). In order to analyze a potential change in collagen organization, a cross-polarized light examination of the Sirius Red-stained area could further quantify the distribution of collagen I and collagen III [29]. Outstandingly, the content of collagen types I and III was significantly upregulated after Ang II infusion under polarizing light microscopy compared with control mice. However, D1KO mice reduced the amount of collagen types I and III compared to WT mice upon Ang II infusion (Fig. 2L and Supplementary Fig. 2D, E). Furthermore, immunohistochemical staining of TGF-β and COL-1 in aortic tissues exhibited similar patterns (Supplementary Fig. S2F-I). Consistent with these observations, fibrosis and collagen deposition decreased in the aortas of mice exposed to Ang II following laminarin treatment (Fig. 2H–M, Supplementary Fig. S2D-I). All the aforementioned results prove that Dectin1 deletion or inhibition ameliorates aortic dysfunction and fibrosis in the Ang II-induced mice.

3.3. Dectin1 exacerbates inflammatory response infusion with Ang II in the mouse aorta

Our previous study demonstrated that Dectin1 facilitated macrophage recruitment, thereby promoting an inflammatory response in heart tissues [23]. Accordingly, we hypothesized that Dectin1 may aggravate aortic inflammatory responses associated with macrophage infiltration. As shown in Fig. 3A–D, Ang II infusion significantly increased the number of co-localized CD68-positive macrophages and Dectin1 and the level of F4/80-positive macrophages compared with the WT controls. However, this increase was completely blocked in the Ang II-challenged D1KO mice. Blood IL-6 and TNF-α levels were then measured, which were markedly increased in the WT mice after Ang II stimulation. In the D1KO mice, the Ang II-induced increments in IL-6 and TNF-α levels were considerably attenuated (Fig. 3E, F). In response to Ang II infusion, we next investigated whether Dectin1 activated the downstream Syk/NF-κB pathway. The higher levels of p-Syk, p-IκB, and nuclear p65 caused by Ang II infusion in WT mice indicated the activation of the Syk/NF-κB pathway in aortic tissues (Fig. 3G and Supplementary Fig. S3A, B). In contrast to WT mice, p-Syk levels and NF-κB activation were significantly down-regulated in D1KO mice after Ang II challenge. Consistently, after being given Ang II, the mRNA levels of *Il6*, *Tnfα*, *Icam1*, *Ccl2*, *Ccl5*, and *Cxcl10* were lower in the aorta of D1KO mice than those of WT mice (Fig. 3H, I). Considering the role of Dectin1 in macrophage phenotypic polarization [23], we investigated this phenotypic alteration in a mouse model of aortic injury induced by Ang II. Immunohistochemical staining results showed that the CD86-positive M1 macrophages were significantly lower, and the

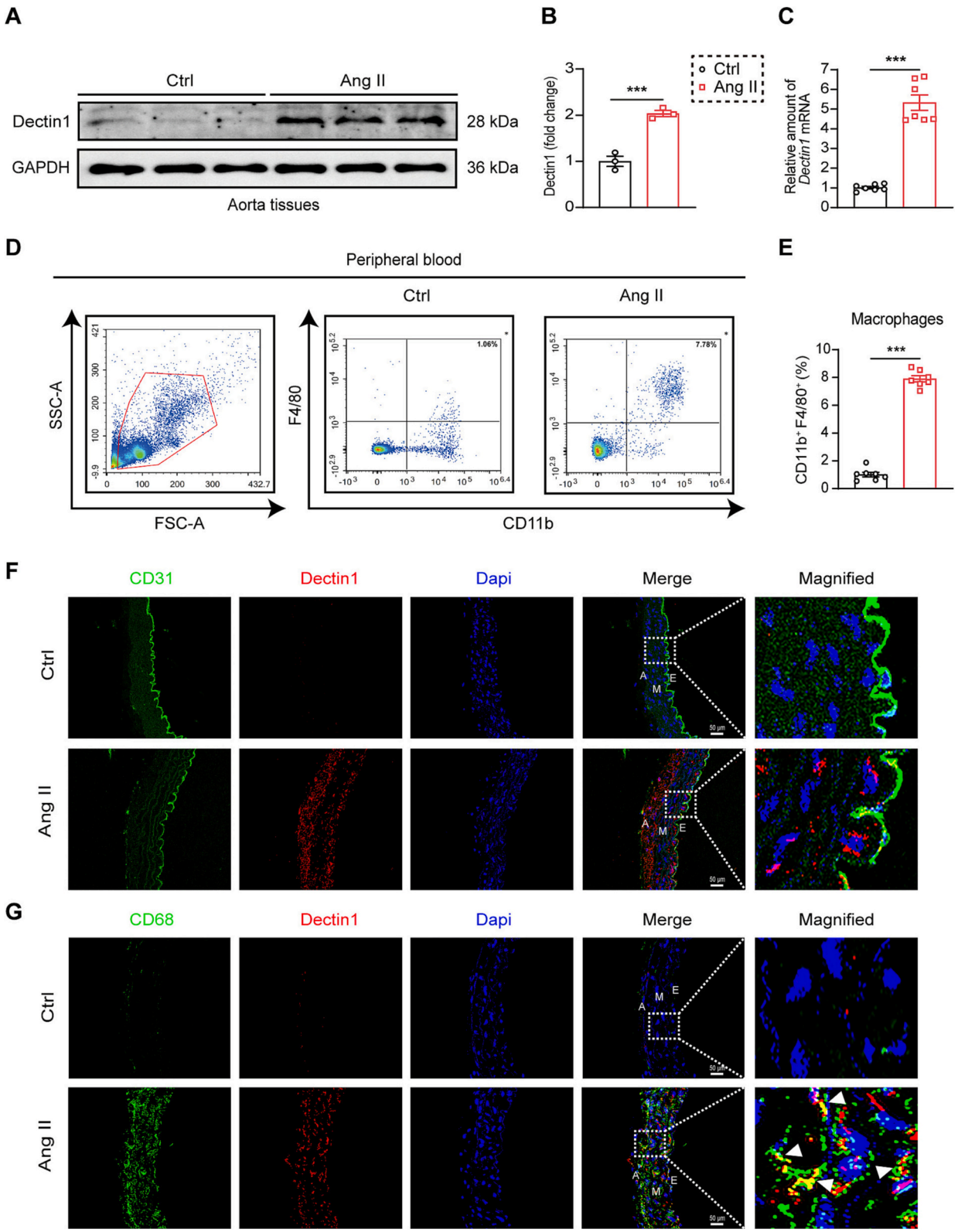

Fig. 1. Dectin1 expression was upregulated, and there was an increase in $CD68^+$ macrophage infiltration in mice injected with angiotensin II (Ang II) in the aorta. (A) Western blotting was performed to assess the Dectin1 protein concentration in the aortic tissues. (B) Quantification of Western blotting results revealed considerably higher levels of Dectin1 in mice stimulated with Ang II compared to that in the control mice ($n = 3$; Mean ± SEM; $^{***}p < 0.001$). (C) RT-qPCR of the Dectin1 mRNA expression in the aortas of control and Ang II-induced mice ($n = 7$; Mean ± SEM; $^{***}p < 0.001$). (D, E) Flow cytometric determination of $CD11b^+$ $F4/80^+$ macrophages in the peripheral blood (n = 7; Mean ± SEM; $^{***}p < 0.001$). (F) Aortic tissues were stained by immunofluorescence for Dectin1 (red) and CD31 (green) (Scale bar = 50 μm). E, endothelium; M, media; A, adventitia. (G) Representative immunofluorescence staining images of the aortic tissues for CD68 (green) and Dectin1 (red), with white arrowheads indicating Dectin1 colocalization with CD68. The tissues were counterstained using DAPI (blue; Scale bar = 50 μm).

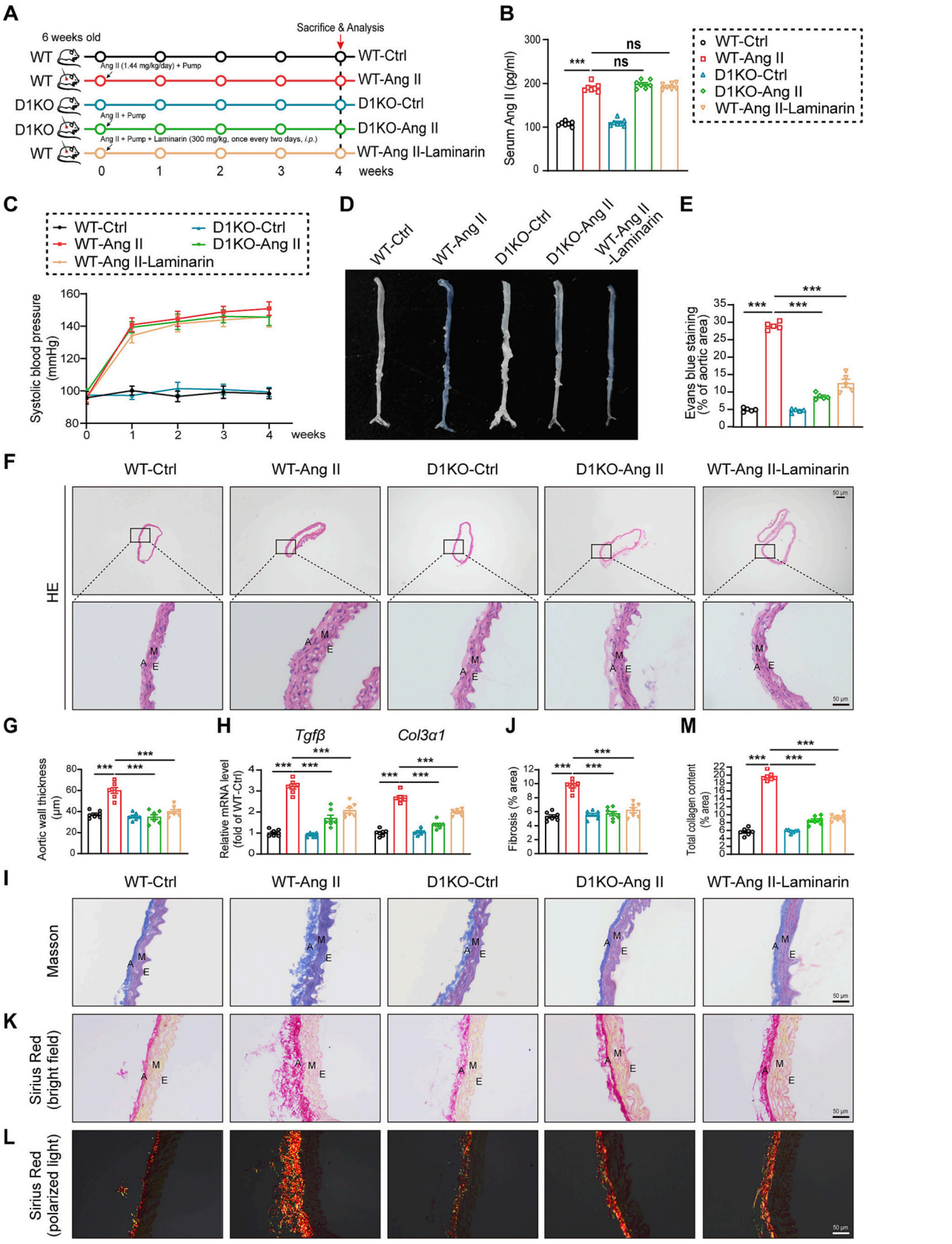

(caption on next page)

Fig. 2. Dectin1 deficiency attenuated angiotensin II (Ang II)-triggered aortic injury and fibrosis in mice. (A) A schematic diagram depicting the animal experiment grouping and procedure. Briefly, the subcutaneous pumps were implanted in wild-type (WT) and Dectin1-knockout (D1KO) mice, releasing Ang II at the rate of 1.44 mg/kg/day for 4 weeks. Laminarin (300 mg/kg), an inhibitor of Dectin1, was administered intraperitoneally every alternate day. Blood and aortic samples were obtained for further analyses. (B) The amount of Ang II in the mouse serum was measured using an ELISA kit ($n = 7$; Mean ± SEM; ns, no significant; ***$p < 0.001$). (C) Periodic systolic blood pressure was determined once a week using a noninvasive tail-cuff pressure analysis system ($n = 7$; Mean ± SEM). (D) The Evans blue-stained areas of the aorta were displayed (E) and quantified ($n = 5$; Mean ± SEM; ***$p < 0.001$). (F, G) H&E staining was performed to determine the thickness of aortic wall. Representative images of the staining are displayed in F (Scale bar = 50 μm). E, endothelium; M, media; A, adventitia. The arterial wall thickness was quantified in (G) (n = 7; Mean ± SEM; ***$p < 0.001$). (H) The mRNA levels of *Col3a1* and *Tgfβ* in the aortic tissues were assessed (n = 7; Mean ± SEM; ***$p < 0.001$). (I) Detection (J) and quantitation of aortic fibrosis in the mice by Masson's trichrome staining (Scale bar = 50 μm; n = 7; Mean ± SEM; ***$p < 0.001$). Representative images of Sirius red-stained aortic tissues showing (K) total collagen deposition under a bright-field microscope (L) and the distribution of type I collagen (red/yellow) and type III collagen (green) using a polarizing microscope (Scale bar = 50 μm). (M) Quantified total collagen deposition of Sirius-red stained sections (n = 7; Mean ± SEM; ***$p < 0.001$).

CD206-positive M2 macrophages were remarkably up-regulated in the aortic sections of D1KO mice compared with WT mice after Ang II treatment (Fig. 3J and Supplementary Fig. S3E-G). Similarly, the RT-qPCR analysis confirmed that M1 pro-inflammatory macrophage markers (*Arg2* and *Inos*) were upregulated and M2 anti-inflammatory macrophage markers (*Arg1* and *Cd206*) had no significant differences in the Ang II-treated WT mice (Supplementary Fig. S3C, D). Conversely, the expressions of *Arg2* and *Inos* were considerably decreased, and the levels of *Arg1* and *Cd206* were elevated in the aortas of the Ang II-treated D1KO mice (Supplementary Fig. S3C, D). Laminarin-induced pharmacological inhibition of Dectin1 yielded similar results. Overall, these findings demonstrate that Dectin1 activation by Ang II induces phosphorylation of Syk and activation of NF-κB, which results in the recruitment of proinflammatory M1 macrophages and an upregulation of proinflammatory cytokines.

3.4. Dectin1 knockout attenuates aortic dysfunction and inflammatory response in DOCA-salt-challenged mice

In order to evaluate the universal significance of our findings, we examined the effect of Dectin1 on DOCA-salt-induced hypertensive aortic damage. A subcutaneous implant of DOCA (50 mg) with 1 % salt in drinking water was given for up to 3 weeks to WT and D1KO mice (Supplementary Fig. S4A). Following a three-week DOCA-salt infusion, increased SBP and DBP were observed in WT mice and D1KO mice (Supplementary Fig. S4B, C). According to H&E staining, DIKO mice showed an observable decrease in aortic wall thickness compared to WT controls induced with DOCA-salt (Supplementary Fig. S4D, E). Masson's trichome staining indicated that the aortic sections observably increased fibrosis in DOCA-salt-induced WT mice, which was greatly attenuated in D1KO mice (Supplementary Fig. S4F, G). Additionally, the D1KO mice showed a clear reversal of the DOCA-salt-induced upregulation of *Tgfβ* and *Col3a1* mRNA levels in WT mice (Supplementary Fig. S4H). Previous research has demonstrated that the DOCA-salt challenge promotes inflammation and macrophage infiltration in aortic tissues [30]. Accordingly, the F4/80-positive areas and the mRNA levels of inflammatory factors (*Il6*), adhesion molecules (*Icam1*), and chemokines (*Ccl2, Cxcl10*) were significantly lower in the D1KO group than in the WT group after DOCA-salt infusion (Supplementary Fig. S4I-L). Furthermore, the mRNA level of *Inos* was significantly increased, but the expression levels of *Cd206* showed no significant difference after DOCA-salt stimulation. In contrast, DOCA-salt-induced effects were fully abolished in D1KO mice (Supplementary Fig. S4M). Similar results were obtained with pharmacological inhibition of Dectin1 induced by laminarin (Supplementary Fig. S4B-M). Therefore, these results show that Dectin1 deletion or pharmacological inhibition ameliorates aortic damage, fibrosis, and inflammatory response in response to DOCA-salt.

3.5. Dectin1 deficiency in myeloid cells suppresses aortic dysfunction in response to Ang II

BMT experiments were conducted to directly verify the exact role of monocyte–macrophage Dectin1 expression in aortic injury. The BM-derived macrophages from the WT mice were intravenously transplanted into the D1KO and WT recipient mice (WT → D1KO and WT → WT), whereas the BM-derived macrophages from D1KO mice were intravenously transferred into the WT and D1KO recipient mice (D1KO → WT and D1KO → D1KO) (Fig. 4A). Tail clip samples, isolated peritoneal macrophages, peripheral blood mononuclear cells, and aortas were used to validate the feasibility of the BMT experiments (Supplementary Fig. S5A-C). Additionally, the SBP and DBP levels showed remarkable increases in both chimeric mice after Ang II infusions for 4 weeks (Supplementary Fig. S5D, E). Subsequently, these mice were stimulated with Ang II infusion for 28 days starting from 3 weeks after adoptive transfer (Fig. 4B). H&E staining of tissues from the Ang II-infused WT mice transplanted with D1KO BM cells revealed a decrease in the aortic wall thickness (Fig. 4C, D). The mRNA levels of fibrosis factors were considerably decreased in D1KO → WT mice caused by Ang II (Fig. 4E). Similarly, Masson's trichrome staining and TGF-β staining revealed reduced aortic fibrosis in the D1KO → WT Ang II-infused mice (Fig. 4G, H; Supplementary Fig. S5F, G). Furthermore, deficiency of the macrophage Dectin1 resulted in decreased expression of inflammatory factors in the aortas of the Ang II-induced D1KO → WT mice, as determined through RT-qPCR and TNF-α staining (Fig. 4F, I; Supplementary Fig. S5H). However, these positive effects were completely reversed in the D1KO mice reconstituted with the WT BM cells. In addition, adoptive transfer of CD68-positive macrophages (green) colocalized with Dectin1 (red) in cross-sections of the aorta in the recipient mouse (Supplementary Fig. S5I, J). All of these results suggest that macrophage Dectin1 activation is crucial for the progression of aortic fibrosis in mice.

3.6. Dectin1 mediates Ang II-induced proinflammatory cytokine production and NF-κB activation in vitro

In view of the apparent functional role of Dectin1 in aortic damage, we investigated the underlying molecular mechanisms through which Dectin1 regulated macrophage pro-inflammatory activation following Ang II induction *in vitro*. Exposure of RAW264.7 cells to 1 μM Ang II for 2 h led to marked upregulation of Dectin1 expression (Fig. 5A; Supplementary Fig. S6A). Additionally, a peak in Syk phosphorylation was observed at 2 h following Ang II induction (Fig. 5B, C). To test the potential association between Dectin1 and inflammatory response in macrophages, Dectin1 was silenced through siRNA transfection of the RAW264.7 cells (Fig. 5D, Supplementary Fig. S6B). Elevated levels of phosphorylated IκBα and the nuclear NF-κB p65 subunit were observed in the Ang II-treated RAW264.7 cells compared with the control cells (Fig. 5E–G). However, Ang II exposure of the Dectin1-silenced cells led to a significant decline in NF-κB activity. In accordance with the findings, Ang II upregulated mRNA expression of several inflammatory factors (*Il6* and *Tnfα*), adhesion factor molecules (*Icam1*), and chemokines (*Ccl2* and *Cxcl10*) in the control RAW264.7 cells but not in the Dectin1-silenced RAW264.7 cells (Fig. 5H, Supplementary Fig. S6C–E). In addition, Dectin1 knockdown resulted in the expression of considerably fewer M1 genes and more M2 markers compared with the Ang II-stimulated RAW264.7 cells (Fig. 5I, J). Similar results were observed

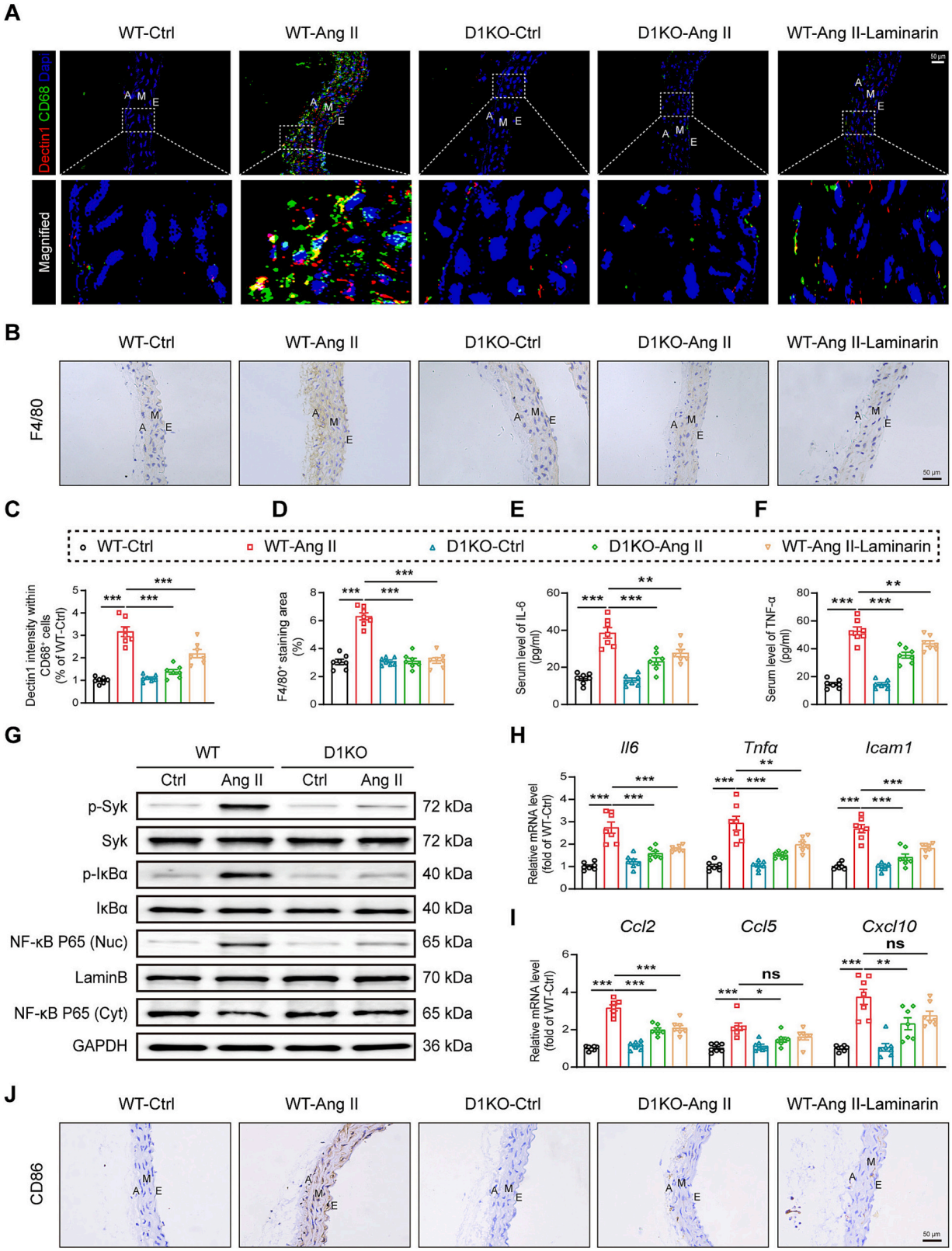

Fig. 3. Dectin1 exacerbated the inflammatory response triggered by angiotensin II (Ang II) in the mouse aorta. (A, C) An illustration of the mouse aorta tissues stained by immunofluorescence displaying the infiltration of CD68 (green) and Dectin1 (red), and counterstaining was performed by DAPI (blue; Scale bar = 50 μm). The fluorescence density values were quantified (n = 7; Mean ± SEM; ***$p < 0.001$). E, endothelium; M, media; A, adventitia. (B, D) The aortic sections were stained with F4/80 (brown; Scale bar = 50 μm). The stained area was quantified (n = 7; Mean ± SEM; ***$p < 0.001$). (E, F) ELISA kits were utilized to determine the levels of IL-6 and TNF-α in the serum obtained from the mice (n = 7; Mean ± SEM; **$p < 0.01$; ***$p < 0.001$). (G) Western blot analysis of p-Syk, p-IκB, cytoplasmic NF-κB p65, and nuclear NF-κB p65 in aortic tissues of the mice. (H, I) The mRNA levels of inflammatory factors (*Il6*, *Tnfα*), adhesion factors (*Icam1*), and chemokines (*Ccl2*, *Ccl5*, *Cxcl10*) in the aortic tissues of mice (n = 7; Mean ± SEM; ns, not significant; *$p < 0.05$; **$p < 0.01$; ***$p < 0.001$). (J) Representative aortic sections stained for M1 macrophage marker CD86 (brown; Scale bar = 50 μm).

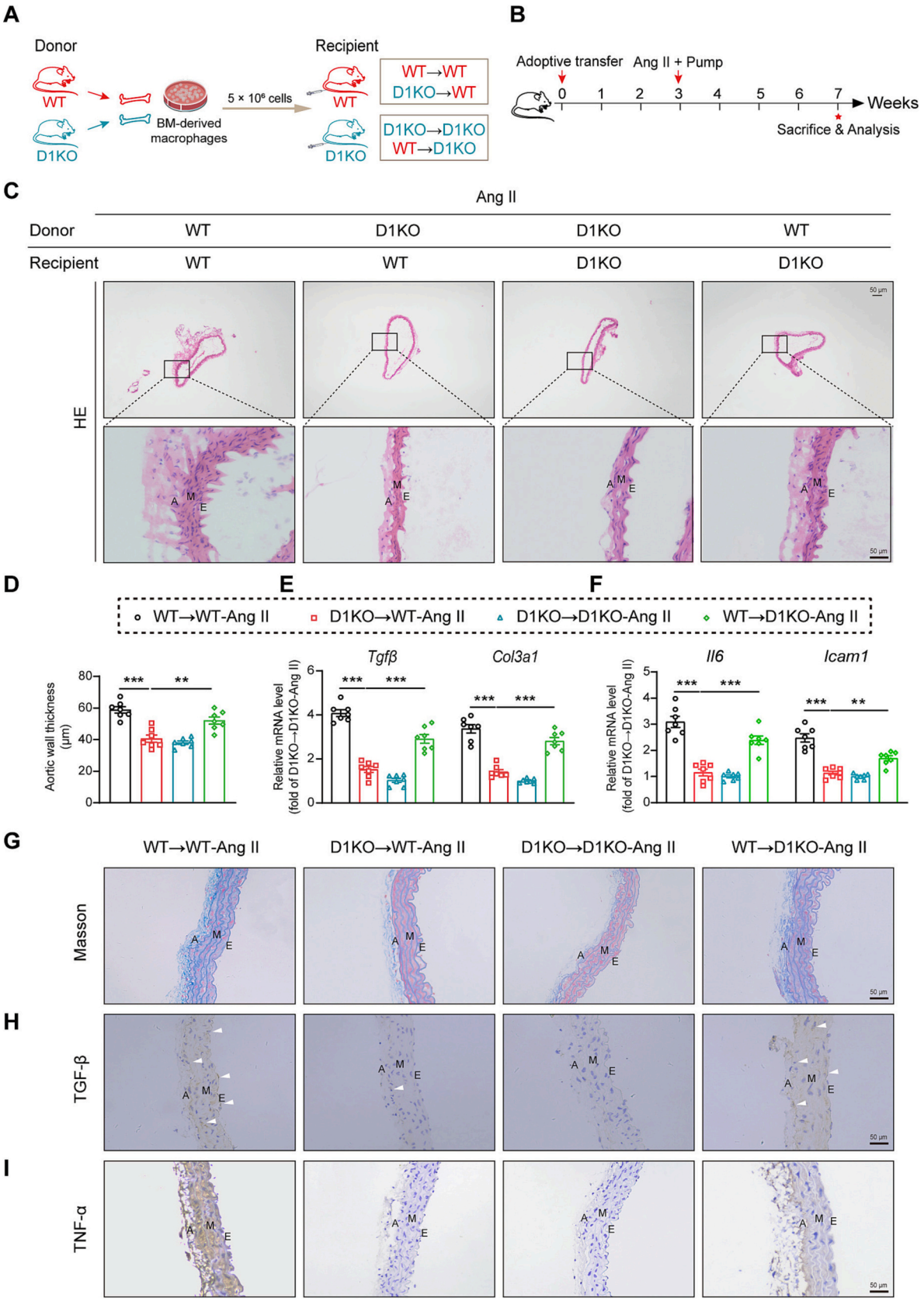

(caption on next page)

Fig. 4. Adoptive transfer of Dectin1-knockout (D1KO) monocytes reversed the aortic inflammatory response and fibrotic phenotype in angiotensin II (Ang II)-infused mice. (A) The protocol for adoptive transfer of the bone marrow (BM)-derived macrophages in Ang II-infusion mouse model. WT → WT: BM-derived cells from WT mice into irradiated WT mice; D1KO → WT: BM-derived cells from D1KO mice into irradiated WT mice; D1KO → D1KO: BM-derived cells from D1KO mice into irradiated D1KO mice; WT → D1KO: BM-derived cells from WT mice into irradiated D1KO mice. (B) Recipient WT and D1KO mice received BM-derived macrophages from donor WT or D1KO mice for 3 weeks. Ang II was administered to 4 groups of recipient mice for 4 weeks. The aortic samples were collected. (C) Representative photos of H&E staining results in the aortic sections (Scale bar = 50 μm). E, endothelium; M, media; A, adventitia. (D) Quantitative analysis of the aortic wall thickness (n = 7; Mean ± SEM; $^{**}p < 0.01$; $^{***}p < 0.001$). (E, F) RT-qPCR analysis of the fibrotic factors (*Tgfβ*, *Col3a1*), inflammatory factor (*Il6*), and adhesion factor (*Icam1*) in the aorta of the adoptive transfer models (n = 7; Mean ± SEM; $^{**}p < 0.01$; $^{***}p < 0.001$). Representative images of Masson's trichrome staining (G), TGF-β staining (H), and TNF-α staining (I), which were used to assess the degree of fibrosis and inflammation in the aortic sections. Positive staining is indicated by white arrows (Scale bar = 50 μm).

through pharmacological inhibition of Dectin1 by using the inhibitor laminarin. The results thus validate that Dectin1-regulated proinflammatory activation of macrophages is mainly facilitated through Syk/NF-κB signaling activation.

4. Discussion

In our latest study, we established that Dectin1 was involved in hypertensive vascular damage and elucidated its underlying molecular mechanism *in vivo* and *in vitro*. The following were the three key findings: (i) Genetic ablation of Dectin1 protected against hypertensive vascular dysfunction, potentially by suppressing macrophage infiltration and pro-inflammatory cytokine production. The same effect was likewise noted in the mice administered with laminarin, a Dectin1 inhibitor. (ii) The BMT experiments further revealed that myeloid-derived Dectin1 facilitated aortic inflammatory injury and collagen deposition. (iii) Mechanistically, Dectin1 promoted macrophage polarization and infiltration by activating Syk/NF-κB signaling pathways *in vivo* and *in vitro* experiments. A graphical abstract has been provided to schematically illustrate the key findings (Fig. 6). Together, these findings provide a fresh insight into the potential of Dectin1 as a therapeutic target for vascular injury-induced cardiovascular disorders.

Inflammation is crucial for the development and maintenance of hypertension-induced cardiovascular damage, involving various immune cells such as T cells and macrophages [31,32]. Given the intricate nature of the immune–inflammatory network, identifying the key regulators of inflammation in hypertension is imperative. Studies have recently demonstrated that elevated Ang II levels trigger immune cell activation and infiltration of adventitial as well as periadventitial adipose tissues [32]. This process can generate numerous pro-inflammatory cytokines and chemokines, thereby accelerating inflammation and promoting hypertensive vascular disease [32–34]. Mikolajczyk et al. [5] also reported that 1,2,3,4,6-penta-O-galloyl-beta-D-glucose regulated perivascular inflammation and prevented vascular dysfunction in hypertension caused by Ang II. Inhibition of vascular inflammatory processes may impede or postpone the progression of hypertensive vascular injury.

The first line of defense for innate immune cells is the identification of damage-associated or pathogen-associated molecular patterns released by stressed or injured tissues *via* pattern recognition receptors, such as C-type lectin receptors (CLRs) [16]. Dectin1, a CLR family member, is distinguished by a type II transmembrane glycoprotein containing an extracellular C-type lectin domain and a single ITAM-like activation motif in the cytoplasmic region [35–37]. Numerous myeloid cells, including the monocyte–macrophage and neutrophil lineages, have considerable Dectin1 expression [38]. Loperena et al. [39] found that Ang II promoted the recruitment of monocytes/macrophages to the kidney and aorta of mice with experimental hypertension. Furthermore, Lin et al. [40] revealed that the adhesion and migration of macrophages contributed to hypertension and vascular dysfunction induced by DOCA-salt. Studies have recently shown that Dectin1 mediates cardiac inflammation and dysfunction during mouse myocardial ischemia–reperfusion injury [22]. Our previous study confirmed that Dectin1 was essential for mediating Ang II-induced inflammation, which subsequently contributed to cardiac remodeling and dysfunction [23]. However, how Dectin1 contributes to hypertension-triggered vascular damage remains uncertain. Consistent with the results of previous studies, Dectin1 was predominantly expressed in CD68-positive macrophages within aortic tissues. Dectin1 expression was considerably upregulated in the aorta and $CD11b^{+}F4/80^{+}$ macrophages in the peripheral blood of the Ang II-infused animals. Additionally, Ang II- or DOCA-salt-induced alterations in the blood pressure of mice were unaffected by the absence of Dectin1, which is a noteworthy finding. Our further data revealed that Dectin1 deletion or pharmacological inhibition effectively attenuated Ang II- or DOCA-salt-challenged aortic fibrosis, macrophage infiltration, and pro-inflammatory cytokine production in mice. These inhibitory effects were confirmed by reconstituting the WT mice with D1KO BM cells. Nevertheless, the precise mechanism through which Dectin1 contributes to hypertensive vascular injury remains ambiguous.

According to earlier studies, Dectin1 regulates inflammation during fungal infections, cancer development, obesity progression, and ischemic stroke [27,41–44]. These pathological signals induce the phosphorylation of the ITAM-like motif of Dectin1, which recruits and activates Syk, a downstream effector molecule. Subsequently, the activation of the NF-κB signal and generation of pro-inflammatory cytokines exacerbate inflammation [19,45]. Ye et al. [23] found that short-term Ang II stimulation induced Dectin1 dimerization as well as the Dectin1/Syk interaction in cultured macrophages. Moreover, *in vitro* studies have distinguished the two distinct macrophage subtypes: conventionally activated M1 macrophages and alternatively activated M2 macrophages. The former macrophages highly express iNOS and secrete inflammatory factors involved in inflammation responses [46]. Of note, Ang II increased Dectin1 expression, phosphorylated Syk, and activated the NF-κB signaling pathway, thereby releasing inflammatory mediators and chemokines *in vivo* and *in vitro*. These changes were reversed with the deletion of Dectin1. The data supported that Dectin1 mediated hypertension-induced M1 macrophage polarization and proinflammatory cytokine production.

However, Szilagyi et al. have found that Dectin1 deficiency did not affect the development of atherosclerosis in an atherosclerotic lesions mouse model by high fat diet [47]. Macrophages Dectin1 may exhibit distinct pathological mechanisms under different pathological states. When the course of the disease reached the stage of atherosclerosis, knockout macrophages Dectin1 may have failed to reverse the pathological state of the disease. Therefore, how the lesion microenvironment coordinates different types of macrophages and its role in the progression of hypertensive vascular injury deserve further exploration.

5. Conclusion

In summary, our study findings suggest that macrophage Dectin1 promotes hypertension-induced vascular injury in mice. Dectin1 deficiency or inhibition mitigates macrophage infiltration, the generation of proinflammatory cytokines, and fibrosis in the Ang II- or DOCA-salt-stimulated mouse aortas. Additional studies conducted using the BMT assay reveal that Dectin1 in myeloid cells is responsible for mediating the aforementioned adverse effects. *In vivo* and *in vitro* studies demonstrate that Dectin1 facilitates Ang II-induced proinflammatory activation of M1 macrophages primarily through the Syk/NF-κB signaling

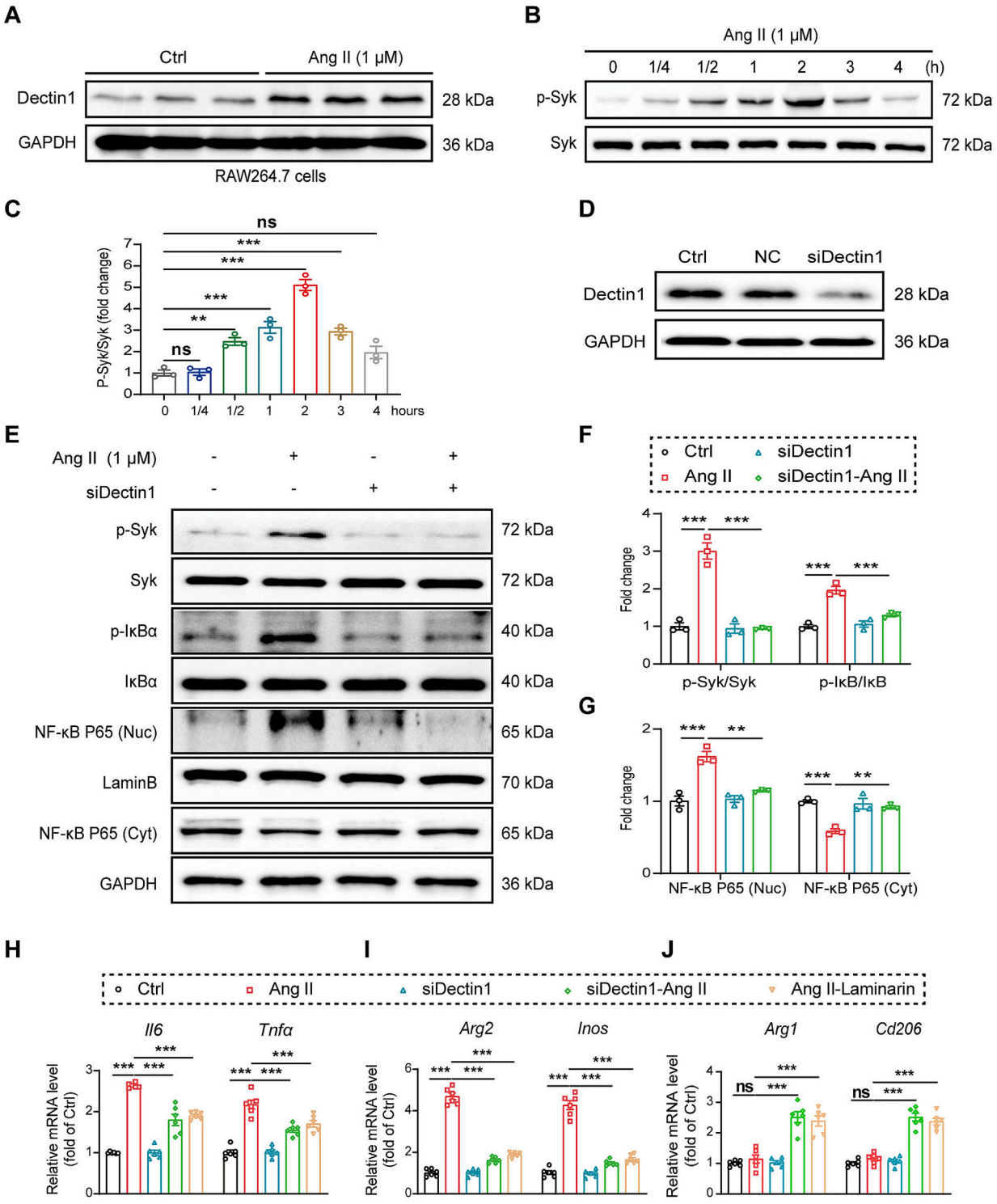

Fig. 5. Dectin1 aggravated inflammatory reactions stimulated by angiotensin II (Ang II) in the macrophages. (A) RAW264.7 cells received stimulation with 1 μM Ang II for 2 h ($n = 3$). The cell lysates were used to analyze the Dectin1 level. (B) RAW264.7 cells were treated with 1 μM Ang II for different durations to detect the p-Syk and Syk expressions, (C) and the densitometric quantification of the representative blots was performed (n = 3; Mean ± SEM; ns, not significant; $^{**}p < 0.01$; $^{***}p < 0.001$). (D) The level of Dectin1 in the RAW264.7 cells was detected after siRNA-mediated silencing (siDectin1) (n = 3). For comparisons, non-transfected (Ctrl) and scrambled (negative control; NC) transfected cells were used. (E–G) Immunoblotting analysis of p-Syk, p-IκB, cytoplasmic NF-κB p65, and nuclear NF-κB p65 in RAW264.7 cells exposed to 1 μM Ang II for 2 h, followed by quantification (n = 3; Mean ± SEM; $^{**}p < 0.01$; $^{***}p < 0.001$). (H) The mRNA levels of *Il6* and *Tnfα* were measured by RT-qPCR ($n = 6$; Mean ± SEM; $^{***}p < 0.001$). (I, J) The mRNA expression of macrophages phenotypic markers in RAW264.7 cells. Markers for M1 macrophages were *Arg2* and *Inos*, while markers for M2 macrophages were *Arg1* and *Cd206* (n = 6; Mean ± SEM; $^{***}p < 0.001$).

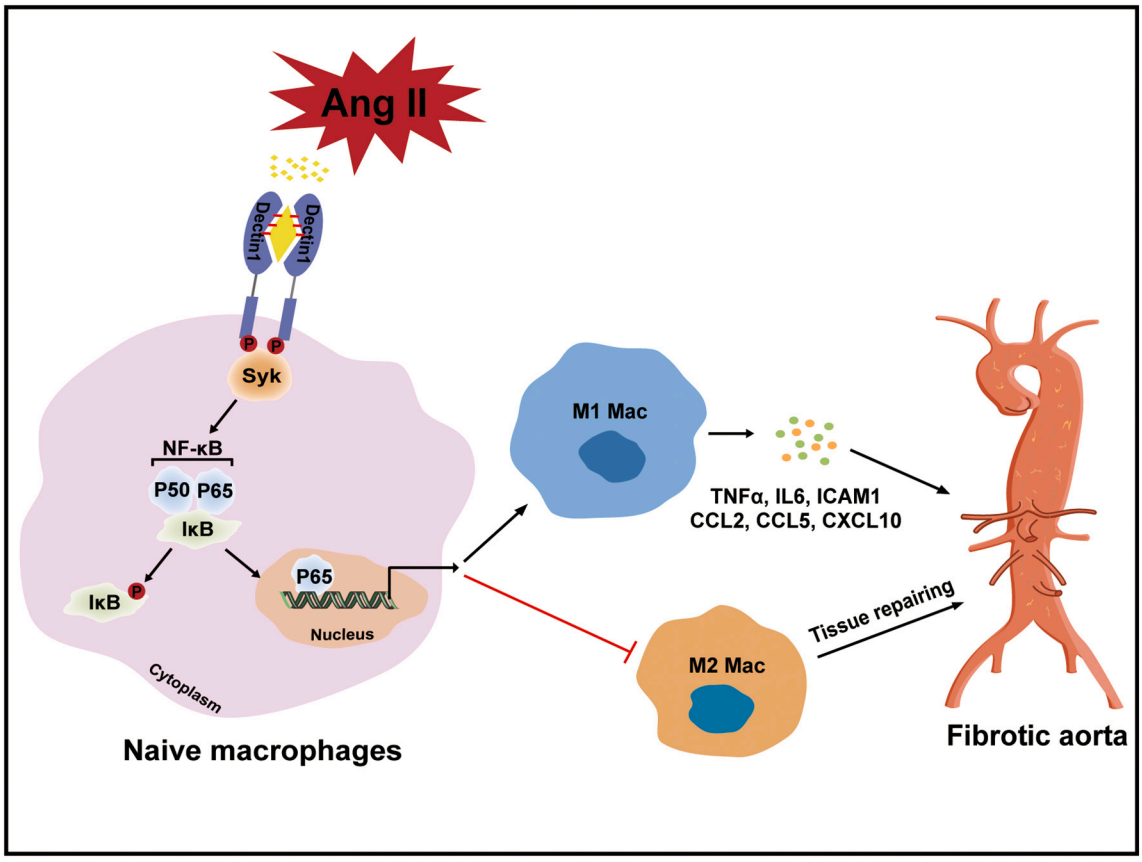

Fig. 6. A schematic diagram depicts a potential mechanism underlying aortic damage caused by angiotensin II (Ang II) in mice. Ang II leads to the homodimerization of Dectin1, which activates the downstream Syk/NF-κB signaling pathway and enhances the generation of inflammatory mediators, chemokines, and adhesion factors from M1 macrophages, resulting in aortic fibrosis in mice.

pathway. Our research results suggest that hypertension-induced vascular injury can be effectively treated by selectively inhibiting Dectin1.

Funds

This study was supported by the National Natural Science Foundation of China (No. 31900381), and Sanming Project of Medicine in Shenzhen (No. SZZYSM202106004).

CRediT authorship contribution statement

Jiajia Zhang: Conceptualization, Formal analysis, Data curation, Writing – original draft, Writing – review & editing. **Yu Tu:** Methodology, Visualization, Writing – review & editing. **Jiajia Wei:** Methodology, Investigation. **Ruyi Zheng:** Data curation. **Ji Shao:** Investigation. **Qinhua Chen:** Investigation, Funding acquisition. **Guang Liang:** Supervision, Project administration, Funding acquisition. **Huazhong Ying:** Supervision, Funding acquisition. **Xue Han:** Conceptualization, Supervision, Writing – review & editing. **Qiaojuan Shi:** Conceptualization, Project administration, Funding acquisition.

Declaration of competing interest

All authors declare no competing financial interest.

Data availability

Data will be made available on request.

Acknowledgments

The authors would like to thank all the reviewers who participated in the review and MJEditor (www.mjeditor.com) for its linguistic assistance during the preparation of this manuscript.

Appendix A. Supplementary data

Supplementary data to this article can be found online at https://doi.org/10.1016/j.bbadis.2023.166911.

References

[1] E.L. Schiffrin, Vascular remodeling in hypertension: mechanisms and treatment, Hypertension 59 (2012) 367–374.
[2] P. Libby, Inflammation in atherosclerosis, Nature 420 (2002) 868–874.
[3] J.A. Chirinos, P. Segers, T. Hughes, R. Townsend, Large-artery stiffness in health and disease, J. Am. Coll. Cardiol. 74 (2019) 1237–1263.
[4] Q.Y. Lin, J. Bai, Y.L. Zhang, H.H. Li, Integrin CD11b contributes to hypertension and vascular dysfunction through mediating macrophage adhesion and migration, Hypertension 80 (2023) 57–69.
[5] T.P. Mikolajczyk, R. Nosalski, D.S. Skiba, J. Koziol, M. Mazur, A.S. Justo-Junior, P. Kowalczyk, Z. Kusmierczyk, A. Schramm-Luc, K. Luc, P. Maffia, D. Graham, A. K. Kiss, M. Naruszewicz, T.J. Guzik, 1,2,3,4,6-Penta-O-galloyl-β-d-glucose modulates perivascular inflammation and prevents vascular dysfunction in angiotensin II-induced hypertension, Br. J. Pharmacol. 176 (2019) 1951–1965.
[6] W. Lieb, D.M. Enserro, L.M. Sullivan, R.S. Vasan, Residual cardiovascular risk in individuals on blood pressure–lowering treatment, J. Am. Heart Assoc. 4 (2015), e002155.
[7] P. Wenzel, M. Knorr, S. Kossmann, J. Stratmann, M. Hausding, S. Schuhmacher, S. H. Karbach, M. Schwenk, N. Yogev, E. Schulz, M. Oelze, S. Grabbe, H. Jonuleit, C. Becker, A. Daiber, A. Waisman, T. Münzel, Lysozyme M–positive monocytes mediate angiotensin II–induced arterial hypertension and vascular dysfunction, Circulation 124 (2011) 1370–1381.

[8] M.S. Madhur, H.E. Lob, L.A. McCann, Y. Iwakura, Y. Blinder, T.J. Guzik, D. G. Harrison, Interleukin 17 promotes angiotensin II–induced hypertension and vascular dysfunction, Hypertension 55 (2010) 500–507.

[9] T.J. Guzik, N.E. Hoch, K.A. Brown, L.A. McCann, A. Rahman, S. Dikalov, J. Goronzy, C. Weyand, D.G. Harrison, Role of the T cell in the genesis of angiotensin II–induced hypertension and vascular dysfunction, J. Exp. Med. 204 (2007) 2449–2460.

[10] T. Basting, E. Lazartigues, DOCA-salt hypertension: an update, Curr. Hypertens. Rep. 19 (2017) 32.

[11] Y. Zhang, J. Bai, W. Yu, Q. Lin, H. Li, CD11b mediates hypertensive cardiac remodeling by regulating macrophage infiltration and polarization, J. Adv. Res. S2090-1232 (2023) 00061–00069.

[12] M.E. Marketou, J.E. Kontaraki, N.A. Tsakountakis, E.A. Zacharis, G.E. Kochiadakis, D.A. Arfanakis, G. Chlouverakis, P.E. Vardas, Arterial stiffness in hypertensives in relation to expression of angiopoietin-1 and 2 genes in peripheral monocytes, J. Hum. Hypertens. 24 (2010) 306–311.

[13] G.D. Brown, P.R. Crocker, Lectin receptors expressed on myeloid cells, Microbiol. Spectr. 4 (2016) 4.5.09.

[14] F. Osorio, C. Reis e Sousa, Myeloid C-type lectin receptors in pathogen recognition and host defense, Immunity 34 (2011) 651–664.

[15] A.M. Kerrigan, G.D. Brown, Syk-coupled C-type lectins in immunity, Trends Immunol. 32 (2011) 151–156.

[16] K. Tone, M.H.T. Stappers, J.A. Willment, G.D. Brown, C-type lectin receptors of the Dectin-1 cluster: physiological roles and involvement in disease, Eur. J. Immunol. 49 (2019) 2127–2133.

[17] D. Daley, V.R. Mani, N. Mohan, N. Akkad, A. Ochi, D.W. Heindel, K.B. Lee, C. P. Zambirinis, G.S.B. Pandian, S. Savadkar, A. Torres-Hernandez, S. Nayak, D. Wang, M. Hundeyin, B. Diskin, B. Aykut, G. Werba, R.M. Barilla, R. Rodriguez, S. Chang, L. Gardner, L.K. Mahal, B. Ueberheide, G. Miller, Dectin 1 activation on macrophages by galectin 9 promotes pancreatic carcinoma and peritumoral immune tolerance, Nat. Med. 23 (2017) 556–567.

[18] X. Li, Y. Bian, P. Pang, S. Yu, X. Wang, Y. Gao, K. Liu, Q. Liu, Y. Yuan, W. Du, Inhibition of Dectin-1 in mice ameliorates cardiac remodeling by suppressing NF-κB/NLRP3 signaling after myocardial infarction, Int. Immunopharmacol. 80 (2020), 106116.

[19] S. Hadebe, F. Brombacher, G.D. Brown, C-type lectin receptors in asthma, Front. Immunol. 9 (2018) 733.

[20] M. Rahabi, G. Jacquemin, M. Prat, E. Meunier, M. AlaEddine, B. Bertrand, L. Lefèvre, K. Benmoussa, P. Batigne, A. Aubouy, J. Auwerx, S. Kirzin, D. Bonnet, M. Danjoux, B. Pipy, L. Alric, H. Authier, A. Coste, Divergent roles for macrophage C-type lectin receptors, dectin-1 and mannose receptors, in the intestinal inflammatory response, Cell Rep. 30 (2020) 4386–4398.e4385.

[21] X. Fu, H. Zeng, J. Zhao, G. Zhou, H. Zhou, J. Zhuang, C. Xu, J. Li, Y. Peng, Y. Cao, Y. Li, H. Chen, L. Wang, F. Yan, G. Chen, Inhibition of dectin-1 ameliorates neuroinflammation by regulating microglia/macrophage phenotype after intracerebral hemorrhage in mice, Transl. Stroke Res. 12 (2021) 1018–1034.

[22] Q. Fan, R. Tao, H. Zhang, H. Xie, L. Lu, T. Wang, M. Su, J. Hu, Q. Zhang, Q. Chen, Y. Iwakura, W. Shen, R. Zhang, X. Yan, Dectin-1 contributes to myocardial ischemia/reperfusion injury by regulating macrophage polarization and neutrophil infiltration, Circulation 139 (2019) 663–678.

[23] S. Ye, H. Huang, X. Han, W. Luo, L. Wu, Y. Ye, Y. Gong, X. Zhao, W. Huang, Y. Wang, X. Long, G. Fu, G. Liang, Dectin-1 acts as a non-classical receptor of Ang II to induce cardiac remodeling, Circ. Res. 132 (2023) 707–722.

[24] S. Ye, W. Luo, Z.A. Khan, G. Wu, L. Xuan, P. Shan, K. Lin, T. Chen, J. Wang, X. Hu, S. Wang, W. Huang, G. Liang, Celastrol attenuates angiotensin II–induced cardiac remodeling by targeting STAT3, Circ. Res. 126 (2020) 1007–1023.

[25] X. Xie, H.L. Bi, S. Lai, Y.L. Zhang, N. Li, H.J. Cao, L. Han, H.X. Wang, H.H. Li, The immunoproteasome catalytic β5i subunit regulates cardiac hypertrophy by targeting the autophagy protein ATG5 for degradation, Sci. Adv. 5 (2019) eaau0495.

[26] T. Failer, M. Amponsah-Offeh, A. Neuwirth, I. Kourtzelis, A. Deussen, V. Todorov, I. Kopaliani, Developmental endothelial locus-1 protects from hypertension-induced cardiovascular remodeling via immunomodulation, J. Clin. Investig. 132 (2022), e126155.

[27] X.C. Ye, Q. Hao, W.J. Ma, Q.C. Zhao, W.-W. Wang, H.H. Yin, T. Zhang, M. Wang, K. Zan, X.X. Yang, Z.H. Zhang, H.J. Shi, J. Zu, H.K. Raza, X.L. Zhang, D.Q. Geng, J. X. Hu, G.Y. Cui, Dectin-1/Syk signaling triggers neuroinflammation after ischemic stroke in mice, J. Neuroinflammation 17 (2020) 17.

[28] H.S. Goodridge, C.N. Reyes, C.A. Becker, T.R. Katsumoto, J. Ma, A.J. Wolf, N. Bose, A.S.H. Chan, A.S. Magee, M.E. Danielson, A. Weiss, J.P. Vasilakos, D.M. Underhill, Activation of the innate immune receptor Dectin-1 upon formation of a 'phagocytic synapse', Nature 472 (2011) 471–475.

[29] I.M. Perea-Gil, C.P. Prat-Vidal, C.D.P. Gálvez-Montón, S.P. Roura, A.P. Llucià-Valldeperas, C.P. Soler-Botija, O.M. Iborra-Egea, I.D.P. Díaz-Güemes, V.D. P. Crisóstomo, F.M.D.P. Sánchez-Margallo, A.M.P. Bayes-Genis, A cell-enriched engineered myocardial graft limits infarct size and improves cardiac function, JACC. Basic Transl. Sci. 1 (2016) 360–372.

[30] C.T. Chan, J.P. Moore, K. Budzyn, E. Guida, H. Diep, A. Vinh, E.S. Jones, R. E. Widdop, J.A. Armitage, S. Sakkal, S.D. Ricardo, C.G. Sobey, G.R. Drummond, Reversal of vascular macrophage accumulation and hypertension by a CCR2 antagonist in deoxycorticosterone/salt-treated mice, Hypertension 60 (2012) 1207–1212.

[31] S.J. Forrester, G.W. Booz, C.D. Sigmund, T.M. Coffman, T. Kawai, V. Rizzo, R. Scalia, S. Eguchi, Angiotensin II signal transduction: an update on mechanisms of physiology and pathophysiology, Physiol. Rev. 98 (2018) 1627–1738.

[32] T.P. Mikolajczyk, P. Szczepaniak, F. Vidler, P. Maffia, G.J. Graham, T.J. Guzik, Role of inflammatory chemokines in hypertension, Pharmacol. Ther. 223 (2021), 107799.

[33] L. Wang, Y.-L. Zhang, Q.-Y. Lin, Y. Liu, X.-M. Guan, X.-L. Ma, H.-J. Cao, Y. Liu, J. Bai, Y.-L. Xia, J. Du, H.-H. Li, CXCL1–CXCR2 axis mediates angiotensin II-induced cardiac hypertrophy and remodelling through regulation of monocyte infiltration, Eur. Heart J. 39 (2018) 1818–1831.

[34] A. Kirabo, V. Fontana, A.P.C. De Faria, R. Loperena, C.L. Galindo, J. Wu, A. T. Bikineyeva, S. Dikalov, L. Xiao, W. Chen, M.A. Saleh, D.W. Trott, H.A. Itani, A. Vinh, V. Amarnath, K. Amarnath, T.J. Guzik, K.E. Bernstein, X.Z. Shen, Y. Shyr, S.-c. Chen, R.L. Mernaugh, C.L. Laffer, F. Elijovich, S.S. Davies, H. Moreno, M. S. Madhur, J. Roberts, D.G. Harrison, DC isoketal-modified proteins activate T cells and promote hypertension, J. Clin. Investig. 124 (2014) 4642–4656.

[35] G.D. Brown, Dectin-1: a signalling non-TLR pattern-recognition receptor, Nat. Rev. Immunol. 6 (2006) 33–43.

[36] K. Ariizumi, G.-L. Shen, S. Shikano, S. Xu, R. Ritter, T. Kumamoto, D. Edelbaum, A. Morita, P.R. Bergstresser, A. Takashima, Identification of a novel, dendritic cell-associated molecule, dectin-1, by subtractive cDNA cloning, J. Biol. Chem. 275 (2000) 20157–20167.

[37] G.D. Brown, S. Gordon, Immune recognition. A new receptor for beta-glucans, Nature 413 (2001) 36–37.

[38] M.E. Deerhake, M.L. Shinohara, Emerging roles of Dectin-1 in noninfectious settings and in the CNS, Trends Immunol. 42 (2021) 891–903.

[39] R. Loperena, J.P. Van Beusecum, H.A. Itani, N. Engel, F. Laroumanie, L. Xiao, F. Elijovich, C.L. Laffer, J.S. Gnecco, J. Noonan, P. Maffia, B. Jasiewicz-Honkisz, M. Czesnikiewicz-Guzik, T. Mikolajczyk, T. Sliwa, S. Dikalov, C.M. Weyand, T. J. Guzik, D.G. Harrison, Hypertension and increased endothelial mechanical stretch promote monocyte differentiation and activation: roles of STAT3, interleukin 6 and hydrogen peroxide, Cardiovasc. Res. 114 (2018) 1547–1563.

[40] Q. Lin, J. Bai, Y. Zhang, H. Li, Integrin CD11b contributes to hypertension and vascular dysfunction through mediating macrophage adhesion and migration, Hypertension 80 (2023) 57–69.

[41] A. Castoldi, V. Andrade-Oliveira, C.F. Aguiar, M.T. Amano, J. Lee, M.T. Miyagi, M. T. Latância, T.T. Braga, M.B. Da Silva, A. Ignácio, J.D. Carola Correia Lima, F. V. Loures, J.A.T. Albuquerque, M.B. Macèdo, R.R. Almeida, J.W. Gaiarsa, L. A. Luévano-Martínez, T. Belchior, M.I. Hiyane, G.D. Brown, M.A. Mori, C. Hoffmann, M. Seelaender, W.T. Festuccia, P.M. Moraes-Vieira, N.O.S. Câmara, Dectin-1 activation exacerbates obesity and insulin resistance in the absence of MyD88, Cell Rep 19 (2017) 2272–2288.

[42] C. del Fresno, D. Soulat, S. Roth, K. Blazek, I. Udalova, D. Sancho, J. Ruland, C. Ardavín, Interferon-β production via dectin-1-Syk-IRF5 signaling in dendritic cells is crucial for immunity to C. albicans, Immunity 38 (2013) 1176–1186.

[43] S. Chiba, H. Ikushima, H. Ueki, H. Yanai, Y. Kimura, S. Hangai, J. Nishio, H. Negishi, T. Tamura, S. Saijo, Y. Iwakura, T. Taniguchi, Recognition of tumor cells by Dectin-1 orchestrates innate immune cells for anti-tumor responses, eLife 3 (2014), e04177.

[44] R.A. Drummond, S. Saijo, Y. Iwakura, G.D. Brown, The role of Syk/CARD9 coupled C-type lectins in antifungal immunity, Eur. J. Immunol. 41 (2011) 276–281.

[45] M. Wagener, J.C. Hoving, H. Ndlovu, M.J. Marakalala, Dectin-1-Syk-CARD9 signaling pathway in TB immunity, Front. Immunol. 9 (2018) 225.

[46] P.J. Murray, Macrophage polarization, Annu. Rev. Physiol. 79 (2017) 541–566.

[47] K. Szilagyi, M.J.J. Gijbels, S. van der Velden, S.E.M. Heinsbroek, G. Kraal, M.P.J. de Winther, T.K. van den Berg, Dectin-1 deficiency does not affect atherosclerosis development in mice, Atherosclerosis 239 (2015) 318–321.